Ultrasonics 53 (2013) 211–218

Contents lists available at SciVerse ScienceDirect

Ultrasonics

journal homepage: www.elsevier.com/locate/ultras

Elastic constants of Ultrasonic Additive Manufactured Al 3003-H18

D.R. Foster [a,*], M.J. Dapino [b], S.S. Babu [a,1]

[a] Department of Materials Science and Engineering, Welding Engineering Program, The Ohio State University, Columbus, OH 43210, USA
[b] Department of Mechanical and Aerospace Engineering, The Ohio State University, Columbus, OH 43210, USA

ARTICLE INFO

Article history:
Received 16 March 2011
Received in revised form 3 March 2012
Accepted 2 June 2012
Available online 17 June 2012

Keywords:
Ultrasonic Consolidation
Ultrasonic testing
Elastic constants
Aluminum alloys
Ultrasonic Additive Manufacturing

ABSTRACT

Ultrasonic Additive Manufacturing (UAM), also known as Ultrasonic Consolidation (UC), is a layered manufacturing process in which thin metal foils are ultrasonically bonded to a previously bonded foil substrate to create a net part. Optimization of process variables (amplitude, normal load and velocity) is done to minimize voids along the bonded interfaces. This work pertains to the evaluation of bonds in UAM builds through ultrasonic testing of a build's elastic constants. Results from ultrasonic testing on UAM parts indicate orthotropic material symmetry and a reduction of up to 48% in elastic constant values compared to a control sample. The reduction in elastic constant values is attributed to interfacial voids. In addition, the elastic constants in the plane of the Al foils have nearly the same value, while the constants normal to the foil direction have much different values. In contrast, measurements from builds made with Very High Power Ultrasonic Additive Manufacturing (VHP UAM) show a drastic improvement in elastic properties, approaching values similar to that of bulk aluminum.

1. Introduction

Ultrasonic Additive Manufacturing (UAM), also known as Ultrasonic Consolidation (UC), is a new manufacturing process in which metallic parts are fabricated from metal foils. The process uses a rotating cylindrical sonotrode to produce high frequency (20 kHz) and low amplitude (20–50 μm), mechanical vibrations to induce normal and shear forces at the interfaces between 150 μm thick metallic foils [1]. The large shear and normal forces are highly localized, breaking up any oxide films and surface contaminants on the material surface, allowing for intimate metal-to-metal contact. As the Ultrasonic Consolidation process progresses, the static and oscillating shear forces cause elastic–plastic deformation and a high dislocation density. The deformation also leads to high localized temperatures through adiabatic heating. The presence of high temperatures and a high dislocation density may trigger recrystallization and atomic diffusion across the interface, leading to a completely solid-state bond [2–4]. This process is repeated, creating a layered manufacturing technique, which continuously consolidates foil layers, to previously deposited material. After every few foil layers, CNC contour milling is used to create the desired part profile with high dimensional accuracy and appropriate surface finishes [5] (see Fig. 1).

The mechanical properties of UAM components are measured using a few testing methods. Peel tests are the most widely used mechanical test as they require only a few consolidated layers (1–3 foil layers), minimal machining and use of a standard mechanical test frame. Peel tests adhere to British Standard EN 2243-2:1991 and involve consolidating foil layers on top of one another with the top most foil being bonded along only half of its length. The top foil layer is then peeled away from the other consolidated foils using a mechanical test frame. Ideally, fracture involves progressively fracturing small colonies of bonded areas along the bonded interface, slowly peeling the interface apart until the entire bonded interface is separated. This test gives the user an interfacial failure load, but often failure occurs through the foil thickness revealing little about the interfacial bond. The interfacial failure load from peel tests can be used to determine optimal UAM process parameters, but cannot be used as a design criterion [6–9].

Traditional tensile and shear tests are also used to evaluate UAM samples. In studies performed by Schick et al. [10] on consolidation of Al 3003-H18, tensile tests revealed that the ultimate tensile strength of UAM samples, with the tensile load oriented in the rolling direction, is 17% greater than monolithic aluminum. Tensile tests with the load orientated in the transverse direction (thickness direction of the foil), revealed that the ultimate tensile strength is 86% less than monolithic aluminum. This suggests that when a UAM component is loaded so that all the interfaces are in the load path (as in the tensile tests in the transverse direction), the strength of UAM components is greatly reduced due to the presence of interfacial voids. Hopkins et al. [11] performed a DOE and statistically characterized the significance of process parameters on the ultimate tensile and shear strength of Al 3003-H18 UAM builds. It was found that vibrational amplitude and normal force

* Corresponding author. Tel.: +1 614 573 6920; fax: +1 614 292 6842.
E-mail addresses: foster.373@osu.edu (D.R. Foster), Babu.13@osu.edu (S.S. Babu).
[1] Tel.: +1 614 247 0001.

0041-624X/$ - see front matter © 2012 Elsevier B.V. All rights reserved.
http://dx.doi.org/10.1016/j.ultras.2012.06.002

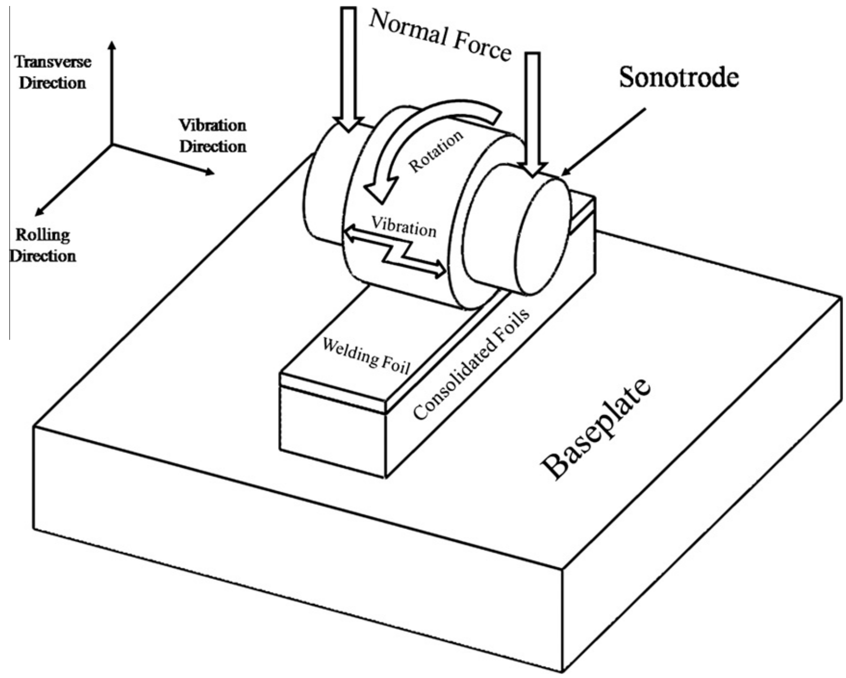

Fig. 1. Schematic of UAM process.

have a strong effect on interfacial bond strength, while welding speed has a relatively weak effect. Even though both Hopkins et al. and Schick et al. performed traditional tensile tests, strain data was not collected; therefore, elastic properties of the UAM specimens were not determined.

The push-pin test is another mechanical test used to evaluate UAM failure load and stiffness. Push-pin tests involve consolidating 16 layers on top of a metal base plate. A hole is then drilled from the bottom of the baseplate through the entire baseplate into the first few foil layers of the UAM build. Then a hardened steel pin is pushed through the stationary baseplate, applying force normal to the consolidated foil, eventually causing delamination or shearing through the foil layers. This method allows for mechanical testing using only a few deposited layers and gives the user a force vs. displacement curve. The push-pin test measures mechanical properties only in the transverse direction and reveals nothing about properties in the vibration and rolling directions. Research by Zhang et al. [12] reported that, because voids are present, the failure loads recorded were much less than with monolithic aluminum and that failure loads increase with increases in bonded area. They also found that the slope of the force vs. displacement curves changed depending on the process parameters, but could not explain why this was occurring.

Although UAM samples were tested using various mechanical testing techniques, macroscopic three-dimensional elastic constants were not determined. Accurate values for elastic constants are needed for modeling the substrate and foil dynamics during consolidation. Modeling of the UAM process has been done by Huang and Ghassemieh [13] as well as Zhang and Li [14]. These authors assume isotropic properties of UAM builds, similar to that of bulk metals, in their models. The isotropy assumption is invalidated by the presence of planes of voids along the bonding interfaces. Prior research has shown that the failure strength of a UAM part depends on the testing direction with respect to foil orientation due to the presence of interfacial voids. Thus, it is likely that interfacial voids not only have an effect on failure strength, but also have an effect on the elastic properties of UAM components. Therefore, the current research focuses on the measurement of the elastic constants in the three material directions (rolling direction, vibration direction and transverse direction) and the characterization of how interfacial voids affect these elastic constants.

To provide context to the current research, a brief review of factors that can lead to a change in the elastic constants of materials is presented below. Considerable change of elastic constants can occur in a material for a number of reasons. Luo and Stevens [15] showed that the Young's and shear moduli of 3Y-TZP ceramics were negatively affected by porosity (e.g. 75% reduction for 38% porosity volume). Kim and Bush [16] demonstrated that decreasing grain size as well as increasing volume fraction of porosity had a negative effect on elastic modulus in Fe, Cu and Pd (e.g. 60% reduction in elastic modulus for 30% porosity volume in Fe). Substantial porosity in these polycrystalline materials had the most prevalent effect on Young's modulus while grain size had a negligible effect unless grain sizes became less than 20 nm. Weertman et al. [17] found that elastic moduli decreased by 66% in nanocrystalline Pd. UAM does not lead to large nanocrystalline regions and therefore, we believe that the microstructure may not have a large effect on elastic constants.

Elastic constants can be measured by mechanical testing. However, due to the small geometries of these builds and lack of yielding, this approach is difficult. In the literature, ultrasonic testing has been used to measure stiffness in the three material directions. Blessing and Bertram [18] used ultrasonic velocity measurements to prove that elastic modulus as well as shear modulus of Al-Alumina composites decrease with porosity. Jeong et al. [19] used ultrasonic testing to determine elastic constants in silicon carbon reinforced aluminum. Thus ultrasonic testing can be used as an alternative to mechanical testing to give accurate elastic constants.

Measuring wave velocities in a material can be used to determine elastic constants. In Fig. 2 side-to-side motions parallel to the incident plane indicate shear wave propagation into the plane. The motions normal to the plane indicate longitudinal wave propagation into the plane. The velocity of each wave is dependent on the material density and directional stiffness. Note the direction coordinate system in which axis-1 is the sonotrode rolling

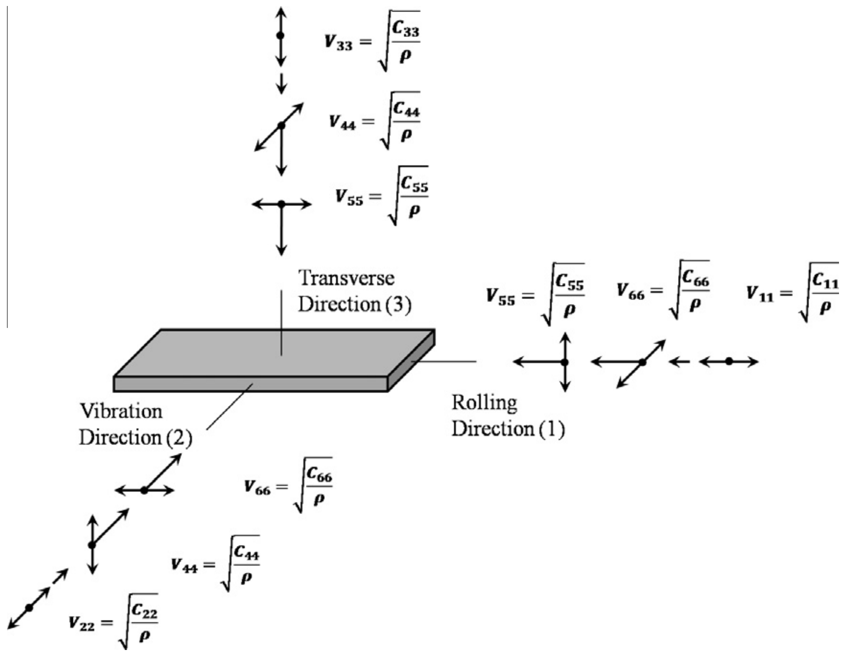

Fig. 2. Schematic of ultrasonic wave propagation in the three material directions.

Table 1
UAM process parameters with respective bond quality.

Sample number	Percentage of bonded area (%)	Linear weld density (%)	Tacking pass			Welding pass		
			Force (N)	Amplitude (μm)	Weld speed (mm/s)	Force (N)	Amplitude (μm)	Weld speed (mm/s)
1	37	75	200	9	51	1000	26	42
2	59	91	200	9	51	1000	26	42
3	65	91	350	12	33	1000	25	28
4	98	98	Not used	Not used	Not used	5500	26	35.5

direction, axis-2 is the sonotrode vibration direction, and axis-3 is the transverse direction. Using the stiffness tensor, the elastic compliance tensor can be calculated using $S_{ij} = (C_{ij})^{-1}$ [20]. These tensors provide relationships between stresses and strains ($\sigma_i = C_{ij}\varepsilon_j$ and $\varepsilon_i = S_{ij}\sigma_j$) and engineering constants G, E, v. Background information regarding using ultrasonic testing to determine elastic constants is available in the literature [21–23].

2. Procedure

The builds constructed in this research used aluminum 3003-H18 foils. Al 3003 is (in weight percentage) 98.6% aluminum, 0.12% copper, and 1.2% manganese and is currently the most widely used material in UAM. The H18 temper designates that the material was cold worked to give a 75% thickness reduction to increase its strength [24]. The aluminum foils (0.15 mm by 23.7 mm cross-section) were fed using a continuous roll during joining.

The process parameters used to create UAM samples with 37%, 59% and 65% bonded areas are listed in Table 1. All builds were made with 149 °C preheat of the substrate. Consolidation for these samples was carried out on the Solidica, Inc. Formation Ultrasonic Consolidation System, which is capable of applying up to 2.2 kN of normal force and 26 μm of vibrational amplitude. The consolidation of each layer was performed using a tacking pass followed by a welding pass on each metallic foil. A single tape width build was used to construct 37% and 65% bonded area builds by continuously depositing one foil on top of the previously deposited foil, as seen in Fig. 3a. The 59% bonded area samples used the same process parameters as that of 37%, except the layering pattern (Fig. 3b) was changed to the "brick wall" layering sequence. In this building sequence, two adjacent foil layers were deposited followed by three adjacent foil layers on top. This pattern was repeated to construct the build. Care was taken so that samples used from the "brick wall" build did not contain foil edges.

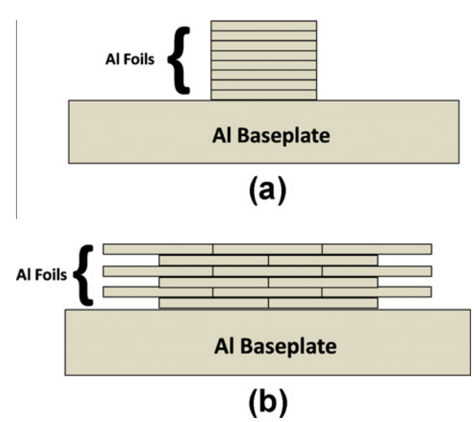

Fig. 3. UAM build configurations. (a) "Single tape width" configuration. (b) "Brick wall" configuration.

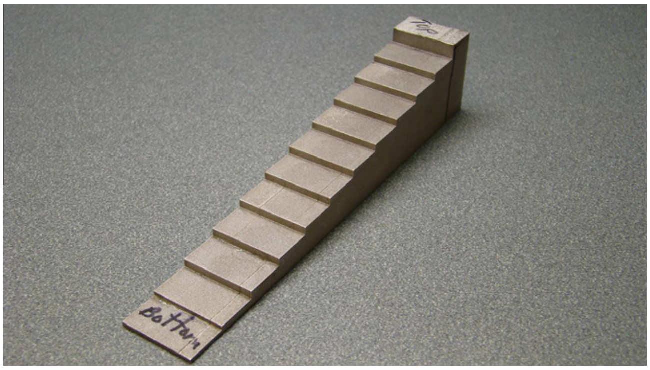

Fig. 4. Picture of step build.

Although similar normal force and amplitude were used for all three samples on the system, reducing the weld speed by 33% and/or changing the stacking sequence caused a change in final percent bonded area of up to 22%. Reducing weld speed allowed for more plastic deformation to occur per unit area because the sonotrode spent more time welding that region. Build sequence likely had an impact on percentage of bonded area because an increase in substrate area, as in the ‘‘brick wall’’ build, requires substantially more force to displace laterally. This is in contrast to the single tape width build which has a small substrate area and requires less relative force to displace it. The greater area of the ‘‘brick wall build’’ allows for more of the ultrasonic energy to be concentrated at the faying surfaces and not lost as mechanical energy into the substrate.

The 98% percent bonded area sample was made using the Very High Powered Ultrasonic Additive Manufacturing (VHP UAM) System produced by Edison Welding Institute and Solidica Inc. This higher-powered Ultrasonic Consolidation system is capable of applying up to 45 kN of normal force and 52 μm of vibrational amplitude. The additional vibrational amplitude and normal force induce a greater amount of plastic deformation at the faying interfaces, compared to the earlier systems (formation UAM system), leading to an increase in bonded area. The VHP UAM system was used to construct a single tape width UAM build without a preheat or tacking pass. The VHP UAM system used is a prototype and is not fully automated, in contrast to the fully automated Formation System. Due to the difficulties of manually aligning and laying foils, the VHP UAM sample height was limited; therefore, only V_{33}, V_{44}, V_{55} measurements could be obtained.

A Krautkramer 58L ultrasonic testing system was used to make ultrasonic phase velocity measurements. A 0.5 in. diameter 2.25 MHz, normal incident, contact, longitudinal wave transducer was used to make longitudinal wave measurements, while a 5 MHz, normal incident, contact, transverse wave transducer was used to make shear wave velocity measurements. The pulse echo method was used to measure wave velocity.

A density value of 2.73 kg/m^3 was used in all stiffness calculations. Density changes due to voids would be minor, affecting only the effective macroscopic stiffness by an estimated 1–3 percent. These changes in stiffness are very small compared to stiffness changes due to changes in the wave velocity which are then squared ($C_{ij} = \rho * V_{ij}^2$). Therefore, density changes due to voids were assumed to be negligible and a literature value of 2.73 kg/m^3 was used for density in calculations of stiffness.

To investigate the potential effect of bond quality on velocity measurements through the thickness of UAM builds, a step sample was constructed with step heights increasing from 2.5 mm to 30 mm (Fig. 4). To create this step build, a 152 mm by 25 mm by 30 mm 59% bonded area UAM block was created in which steps of increasing height were cut using EDM. Wave velocity was measured along the transverse direction of each step. Changes in measured velocity at different steps would be an indication that the bonded areas varied throughout the depth.

‘‘Percentage of bonded area’’ was used instead of ‘‘Linear weld density’’ (LWD) to evaluate the amount of bonding at the welding interface. The LWD measurements use a cross-section of a UAM

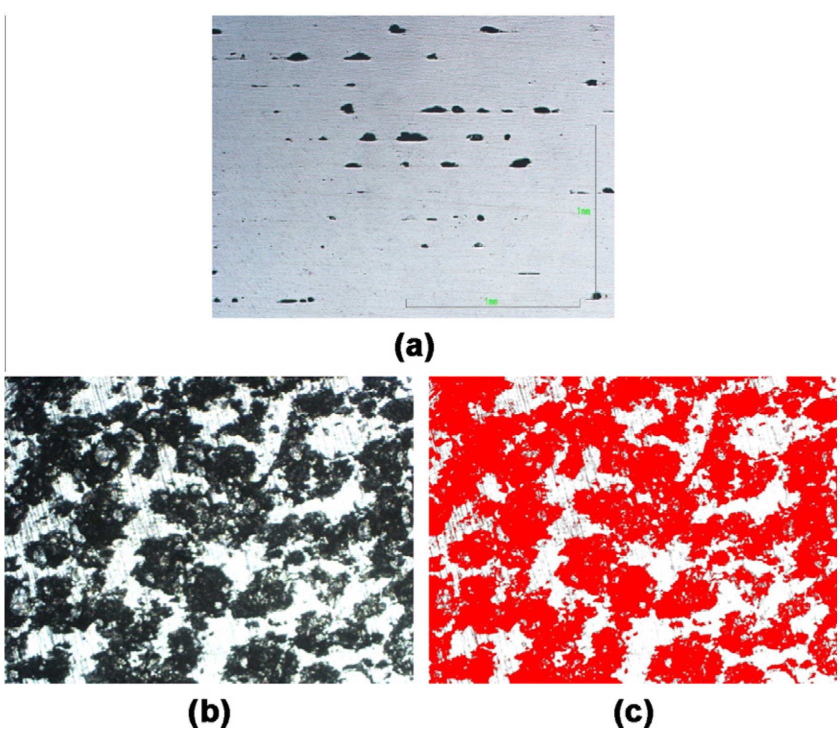

Fig. 5. (a) Cross-section of UAM build. (b) UAM fracture surface. (c) Image threshold measurement of UAM fracture surface using Fiji imaging software.

build, as seen in Fig. 5a. Comparing the length of voids at the interfaces to the total length of the interface, the amount of bonding (LWD) can be measured. This method of evaluation can be subjective with adjacent interfaces displaying a range of bonded values [25]. "Percentage of bonded area" measurements evaluate interface bonding by surveying fracture surfaces (Fig. 5b). Bonded areas are deformed and have greater heights than unbonded areas. Because this type of measurement has been shown to be more repeatable and accurate than LWD [11], it was chosen to be the primary technique used to determine the amount of interfacial bonding. To measure percent bonded area, high contrast images of the fracture surface were taken with a Meijer optical microscope. Then Fiji image processing software [26] was used to determine a suitable contrast threshold in which bonded areas would be highlighted due to their darker appearance (Fig. 5c). Once an appropriate threshold was found, the area fraction of the highlighted sections was used as the "Percentage of bonded area" measurement. The VHP UAM sample could not be constructed to a suitable height to be fractured in order to obtain a Percentage of bonded area measurement; consequently LWD was measured and assumed to be the same as percentage of bonded area for that sample.

3. Results and discussion

3.1. Step build

Measured velocities from the step build are displayed in Fig. 6. Neither longitudinal (V_{33}) nor shear (V_{55}) velocity measurements on the step build show significant change with step height. This observation suggests that the amount of bonded area (and therefore stiffness) does not vary significantly with build height. The minimum UAM thickness needed to obtain accurate measurements is 5 mm, which is consistent with recommendations from ASTM standard E494 [27]. V_{33} could be measured up to 23 mm before scattering of the ultrasonic waves due to the voids prevented velocity measurements, while V_{55} could be measured at all step heights above 5 mm.

3.2. Characterization of control sample

The foils used for UAM have a H18 temper designation. Under H18 designation, the initial annealed aluminum was cold rolled to a reduction in thickness of 75%. Cold rolling can affect material properties, causing mechanical properties to be different in each material direction. To ensure that the stiffness of UAM samples was not due to the initial condition, an Al 3003-H14 "control sample" was ultrasonically tested. Although the H14 temper is not cold worked to the degree of H18 temper (50% thickness reduction compared to 75% thickness reduction), it can provide stiffness values that are close to those of Al 3003-H18 foil. In addition, measurements from the control sample could elucidate whether or not observed stiffness changes in UAM builds were due to the initial rolled state of the foil.

The Al 3003-H14-control sample had slightly higher elastic constant values compared to literature values for Al 3003 [24] for all elastic constants except C_{66} (see Table 2). The largest difference was in C_{11}, C_{22}, and C_{33} which had changes of 12%, 9% and 6%. C_{44}, C_{55}, and C_{66} differed from literature values by a maximum of 3%. The slightly larger constants obtained for C_{44}, C_{55}, and C_{66} are within acceptable experimental error (±4%), but comparison of the C_{11}, C_{22} and C_{33} cases show significantly higher stiffness constants even when measurement errors are considered. Overall, cold rolling Al 3003 has a slight stiffening effect on the material.

3.3. Characterization of UAM samples

Knowledge of material symmetries can be effectively used to reduce the number of independent constants in a material's stiffness tensor. To test for orthotropic symmetry, V_{44} was tested in the vibration and transverse directions, V_{55} was tested in the rolling and transverse directions and V_{66} in the rolling and vibration directions (see Fig. 2). V_{44}, V_{55} and V_{66} each had the same velocity in both of the directions tested. This result indicates at least

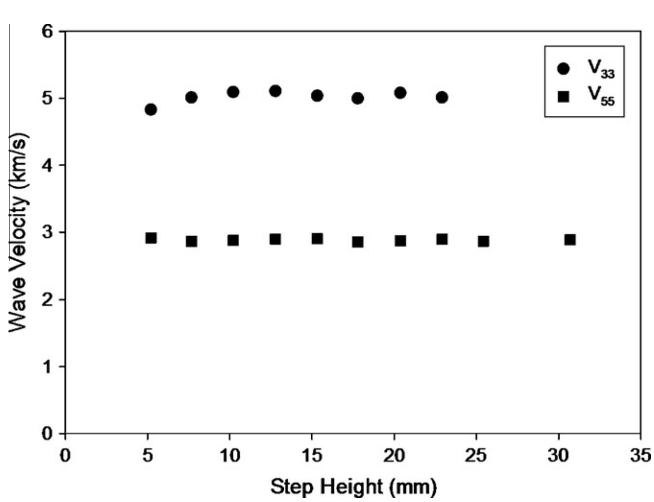

Fig. 6. Wave velocity vs. build height for the step build.

Table 2
Comparison of elastic constants between isotropic and cold worked Al 3003.

	Literature value Al 3003-H18 (GPa)	Al 3003-H14 (GPa)	Difference between Al 3003-H14 and isotropic Al 3003 (%)
C_{11}	102	115.7	12
C_{22}	102	112.6	9
C_{33}	102	108.9	6
C_{44}	25.9	26.1	1
C_{55}	25.9	26.1	1
C_{66}	25.9	25.2	−3

Table 3
Comparison of elastic constants for 37% bonded area UAM samples.

	Al 3003-H14 (GPa)	UT testing of 37% bonded area UAM sample (GPa)	Difference between Al 3003-H14 and UAM samples (%)
C_{11}	115.7	92	−20
C_{22}	112.6	94.6	−16
C_{33}	108.9	53.3	−51
C_{44}	26.1	18.1	−31
C_{55}	26.1	18.1	−31
C_{66}	25.2	25	−1

Table 4
Comparison of elastic constants for 59% bonded area UAM samples.

	Al 3003-H14 (GPa)	UT testing of 59% bonded area UAM sample (GPa)	Difference between Al 3003-H14 and UAM samples (%)
C_{11}	115.7	99.5	−14
C_{22}	112.6	100.2	−11
C_{33}	108.9	68.8	−37
C_{44}	26.1	19.9	−24
C_{55}	26.1	20.6	−21
C_{66}	25.2	25.8	2

Table 5
Comparison of elastic constants for 65% bonded area UAM samples.

	Al 3003-H14 (GPa)	UT testing of 65% bonded area UAM sample (GPa)	Difference between Al 3003-H14 and UAM samples (%)
C_{11}	115.7	96.7	−16
C_{22}	112.6	99.5	−12
C_{33}	108.9	78.2	−28
C_{44}	26.1	23.4	−10
C_{55}	26.1	23.1	−11
C_{66}	25.2	25	−1

orthotropic symmetry in UAM components and that V_{44}, V_{55}, and V_{66} could be measured in two different material directions. Assuming at least an orthotropic material symmetry, elastic constants in UAM builds were measured.

Elastic constants for UAM samples with 35%, 59% and 65% bonded areas are compared to the Al 3003-H14-control sample in Tables 3–5. In almost all cases the UAM material had lower elastic constant values than the control material. The disparity between UAM samples and the control sample decreased as the percentage of bonded area increased.

The difference in elastic constant values between the control sample and UAM samples in Tables 3–5 is especially large for C_{33}, C_{44} and C_{55}. In the case of the 37% bonded area sample, each of these constants displayed a reduction between 31–51% compared to the control sample. The magnitude of measured elastic constants in the UAM builds increased with an increase in bonded area. For the case of 59% bonded area, there was a reduction in elastic constants of 23–37% vs. control and in the case of 65% bonded area, there was a reduction in elastic constants between 10–28% vs. control.

Constants C_{11}, C_{22}, and C_{66} also had a reduction in value that was dependent on percentage of bonded area, but their reduction was not as severe as that of C_{33}, C_{44}, and C_{55}. At 37% bonded area, the UAM samples had a 1–20% difference in C_{11}, C_{22} and C_{66} compared to the control. As the percentage of bonded area increased for these constants, the discrepancy in elastic constant values between UAM and control results reduced with a maximum of 14% reduction in the case of 59% bonded area and maximum of 16% reduction in the case of 65% bonded area. In all UAM builds stiffness components in the rolling and vibration directions are very similar. C_{11} and C_{22}, along with C_{44} and C_{55} in each case have values that are within 3.5% of each other.

The elastic constants in the VHP UAM sample were not significantly affected by the presence of voids, due to 98% bonded area, and therefore, had similar properties to those of the control sample. There was a 0.5% difference in C_{33} and a 7% difference in C_{44} and C_{55} compared to control, as seen in Table 6. Although elastic constants in the other material directions could not be tested, it is likely that those properties would be close to those of the control sample. This is due to material properties in the rolling and vibration direction being less severely affected by voids at the interfaces when compared to the transverse direction. Since the VHP UAM sample demonstrates that the properties in the transverse direction are similar to those of the control, the properties in the rolling

Table 6
Comparison of elastic constants for 98% bonded area UAM samples.

	A1 3003–H14 (GPa)	UT testing of 98% bonded area VHP UAM sample (GPa)	Difference between Al 3003-H14 and VHP UAM sample (%)
C_{33}	108.7	109.2	0.5
C_{44}	26.1	28.1	7
C_{55}	26.1	28.1	7

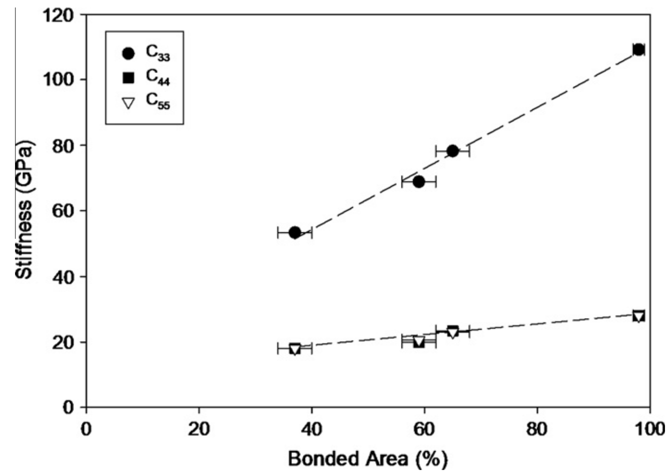

Fig. 7. Stiffness vs. percentage of bonded area.

and vibration directions are likely also close to those of the control. These results indicate that the multidirectional stiffness of the VHP UAM sample material is likely very close to that of the Al foils used to construct the sample.

Stiffness values for C_{33}, C_{44} and C_{55} from Tables 2–6 are plotted in Fig. 7. The effective stiffness decreases linearly with a decrease in percentage of bonded area. The data from VHP UAM supports this observation. As a result of the linear relationship between percentage of bonded area and stiffness, bond quality of UAM components can be determined non-destructively. By measuring stiffness and relating that value to a reference curve, such as Fig. 7, bond quality of a UAM part can be determined. The linear relationship between stiffness and percentage of bonded area is of great importance because it allows UAM parts to be characterized on the shop floor soon after consolidation without the need for time consuming cutting, polishing and optical microscopy.

LWD and percentage of bonded area are compared in Table 1. LWD measurements indicate a much higher degree of bonding compared to the percentage of bonded area measurements. The 37% bonded area sample had a 75% LWD, the 59% bonded area sample had a 91% LWD and the 65% bonded area sample had a 91% LWD. Stiffness vs. LWD for C_{33}, C_{44} and C_{55} area are plotted in Fig. 8. The resulting linear trend between stiffness and LWD is much poorer than that between stiffness and percentage of bonded area in Fig. 7. Plotting stiffness vs. LWD results in a linear trend

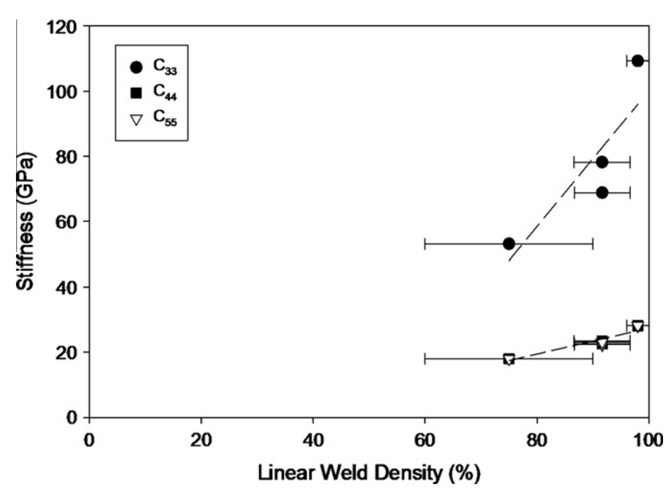

Fig. 8. Stiffness vs. LWD.

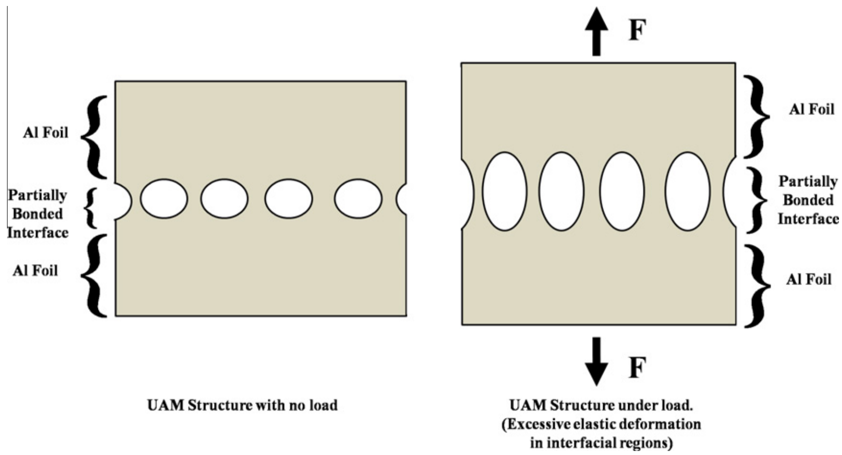

Fig. 9. Schematic of UAM response to loading.

with large deviations from the trend line while stiffness vs. percentage of bonded area plot follows the linear trend much more closely.

It is hypothesized that the change in material stiffness is due to the presence of voids at the welding interface. These void volumes are filled with no matrix material and thus have negligible mass and strength. As a result, when the material is loaded, the bulk foil portion of the UAM part elastically deforms a small amount, while the interface region under the same load will deform more. This is because the load bearing cross-sectional area at the interface is smaller due to the presence of the voids for a given load (Fig. 9). The combined loading response from the bulk foils and interface region results in an overall greater elastic deformation of the part for a given load. This phenomenon creates a component with an effective stiffness that is lower than the foils used to construct it.

The elastic deformation of an UAM part is analogous to springs in parallel and series. C_{33}, C_{44} and C_{55} relate to the stiffness of a part when the partially bonded interfaces are in the load path, while elastic constants C_{11}, C_{22} and C_{66} relate to the material stiffness when the interfacial region is parallel to the load path. When spring elements are in series, like in the case of C_{33}, C_{44} and C_{55}, all elements are in the load path and experience the same load but displace different amounts based on their stiffness. The lower stiffness interfacial regions elastically deform a greater amount than the foil regions, resulting in parts with less effective stiffness in those directions. When spring elements are parallel, as in the case of C_{11}, C_{22} and C_{66}, the interfacial regions a well as the bulk foil regions displace the same amount. However, most of the load is carried by the bulk regions of the foil and not by the partially bonded region. This is the reason there is a smaller stiffness reduction in the rolling and vibration directions compared to the transverse direction.

This discovery of lower effective stiffness and directionally dependent stiffness is of great importance. Accurate elastic constants are needed to model the UAM process as well as to adopt UAM parts in general engineering design. For example, modeling the lateral displacement of a large UAM build due to the shear forces caused by a sonotrode has been elusive. This tendency has been used to rationalize the process's inability to make UAM builds above a critical height. Modeling such phenomena would need an accurate shear modulus in the vibration direction, which is C_{44} ($C_{44} = G_{23}$). If one would compare stress results using 37% bonded area G_{23} (18.1 GPa) to isotropic G (25.9 GPa), there would be a measurement error of 31%. This large error in calculations could lead to simulation results that do not accurately describe response to loads that UAM parts experience.

4. Conclusions

Parts made by Ultrasonic Additive Manufacturing were evaluated with ultrasonic testing. Wave velocity, percentage of bonded area and material stiffness do not change significantly with build height.

The effective stiffness of Al 3003-H18 UAM parts was reduced due to the presence of voids. When a load is applied, the interfacial welded regions that contain voids elastically deform more than the bulk foil regions, resulting in an overall reduction in effective stiffness compared to monolithic aluminum. The reduction in stiffness components can be as high as 51% in the transverse direction while up to only 20% in the rolling and vibration directions. Material properties in the rolling and vibration directions are approximately the same (maximum of 3.5% difference) while the material properties in the transverse direction are much different. The elastic constants measured in samples made by VHP-UAM processing were close to those of monolithic aluminum. The cold worked state of the Al 3003 foils used in UAM is not the cause of stiffness reduction in Al 3003 UAM parts. Cold working Al 3003 increases elastic constant values by as much as 12% in H14 state. Material velocity measurements can be used as a non-destructive test to evaluate bond quality UAM builds.

Acknowledgements

The authors would like to thank Christopher Hopkins, Ryan Hahnlen, and Sriraman Ramanujam of Ohio State University as well as Matt Short, Mark Norfolk and Karl Graff of Edison Welding Institute (EWI) for their input on the project. Financial support for this research was provided by the Ohio Space Grant Consortium (OSGC) and an Ohio Department of Development Wright Project.

References

[1] D.R. White, Ultrasonic consolidation of aluminum tooling, Advanced Materials and Processes 161 (2003) 64–65.
[2] R.L. O'Brien, Ultrasonic welding, in: Welding Handbook, American Welding Society, 1991, pp. 783–812.
[3] R.R. Dehoff, S.S. Babu, Characterization of interfacial microstructures in 3003 aluminum alloy blocks fabricated by ultrasonic additive manufacturing, Acta Materialia 58 (2010) 4305–4315.
[4] H. Fujii, M.R. Sriraman, S.S. Babu, Quantitative evaluation of bulk and interface microstructures in Al 3003 alloy builds made by very high power ultrasonic additive manufacturing, Metallurgical and Materials Transactions A 42 (2011) 4045–4055.
[5] G.D. Janaki Ram, C. Robinson, Y. Yang, B.E. Stucker, Use of ultrasonic consolidation for fabrication of multi-material structures, Rapid Prototyping Journal 13 (2007) 226–235.

[6] C.Y. Kong, R.C. Soar, P.M. Dickens, Characterisation of aluminium alloy 6061 for the ultrasonic consolidation process, Material Science and Engineering A 363 (2003) 99–106.
[7] R.J. Friel, K.E. Johnson, P.M. Dickens, R.A. Harris, The effect of interface topography for ultrasonic consolidation of aluminum, Material Science and Engineering A 527 (2010) 4474–4483.
[8] C.Y. Kong, R.C. Soar, P.M. Dickens, Optimum process parameters for ultrasonic consolidation of 3003 aluminum, Journal of Materials Processing Technology 146 (2004) 181–187.
[9] D. Li, R.C. Soar, Optimum process parameters and influencing factors for embedding SiC Fibers in Al 6061 O matrix through ultrasonic consolidation, in: Material Science and Technology, MS&T Partner Societies, Detroit, Michigan, USA, 2007, pp. 3048–3064.
[10] D.E. Schick, R.M. Hahnlen, R. Dehoff, P. Collins, S.S. Babu, M.J. Dapino, J.C. Lippold, Microstructural characterization of bonding interfaces in aluminum 3003 blocks fabricated by ultrasonic additive manufacturing, Welding Journal 89 (2010) 105–115.
[11] C.D. Hopkins, P.J. Wolcott, M.J. Dapino, A.G. Truog, S.S. Babu, S.A. Fernandez, Optimizing ultrasonic additive manufactured Al 3003 properties with statistical modeling, Journal of Engineering Materials and Technology 134 (2012) 011004. 011001–011038.
[12] C.S. Zhang, A. Deceuster, L. Li, A method for bond strength evaluation for laminated structures with application to ultrasonic consolidation, Journal of Materials Engineering and Performance 18 (2009) 1124–1132.
[13] C.J. Huang, E. Ghassemieh, 3D coupled thermomechanical finite element analysis of ultrasonic consolidation, Material Science Forum 539–543 (2007) 2651–2656.
[14] C.S. Zhang, L. Li, Effect of substrate dimensions on dynamics of ultrasonic consolidation, Ultrasonics 50 (2010) 811–823.
[15] J. Luo, R. Stevens, Porosity-dependence of elastic moduli and hardness of 3Y-TZP ceramics, Ceramics International 25 (1999) 281–286.
[16] H.S. Kim, M.B. Bush, The effects of grain size and porosity on the elastic modulus of nanocrystalline materials, Nanostructured Materials 11 (1999) 361–367.
[17] G.W. Nieman, J.R. Weertman, R.W. Siegel, Mechanical behavior of nanocrystalline metals, in: Acta Metallurgical Conference: "Materials with Ultrafine Microstructures", Atlantic City, NJ USA, 1990.
[18] G.V. Blessing, A.L. Bertram, Elastic moduli of porous metal composites, in: Ultrasonic Symposium 1979, pp. 332–335.
[19] H. Jeong, D.K. Hsu, R.E. Shannon, P.K. Liaw, Charaterization of anisotrpoic elastic constants of silicon–carbon particulate reinforced aluminum metal matrix composites, Part 1. Experiment, Metallurgical and Materials Transactions A 25A (1994) 799–809.
[20] G.H. Staab, Laminar Composites, Butterworth-Heinemann, 1999.
[21] J. Szilard, Ultrasonic Testing: Non-Conventional Testing Techniques, John Wiley & Sons, 1982.
[22] J.D.N. Cheeke, Fundamentals and Application of Ultrasonic Waves, CRC Press LLC, 2002.
[23] B.A. Auld, Acoustic Fields and Waves in Solids, Krieger Publishing Company, 1990.
[24] J.W. Bray, ASM Handbooks Online, vol. 2, ASM International, 1990. pp. 29–61.
[25] C.D. Hopkins, Development and characterization of optimum process parameters for metallic composites made by ultrasonic consolidation, in: Mechanical Engineering, The Ohio State University, Columbus, 2010.
[26] W. Rasband, J. Schindelin, A. Cardona, FIJI, in: pacific.mpi-cbg.de, 2010.
[27] ASTM, Standard Practice for Measuring Ultrasonic Velocity in Materials, E494-10-ASTM International, 2001.